East European Journal of Physics. **2.** 187-190 (2023)
DOI:10.26565/2312-4334-2023-2-19 ISSN 2312-4334

SOME PROPERTIES OF SEMICONDUCTOR-FERROELECTRIC STRUCTURES[†]

Zakirjan T. Azamatov, Sharifa B. Utamuradova, Murodjon A. Yuldoshev*, Nurlan N. Bazarbayev
Institute of Semiconductor Physics and Microelectronics, National University of Uzbekistan,
20 Yangi Almazor st., Tashkent, 100057, Uzbekistan
**Corresponding Author e-mail: murod.yuldoshev1993@gmail.com*
Received March 17, 2023; revised March 27, 2023; accepted March 29, 2023

This paper presents the properties of semiconductor-ferroelectric structures consisting of ZnO nanorods grown at low temperatures by the hydrothermal method on $LiNbO_3$ and $LiNbO_3$:Fe substrates. The resulting structures were analyzed by scanning electron microscope, photoluminescence, and spectrophotometry. SEM images and spectra; absorption spectra; photoluminescence spectra in the ultraviolet and visible ranges are presented. The studies have shown the possibility of using, along with others, the hydrothermal method for the synthesis of $Zn(NO_3)_26H_2O$ and $C_6H_{12}N_4$ to obtain arrays of ZnO nanorods as a sensitive element of surfactant-based UV radiation sensors.
Keywords: *nanorod; photoluminescence; scanning electron microscope; absorption spectrum*
PACS: 68.37.Hk, 78.55.Ap, 42.25.Bs, 61.46.Km

INTRODUCTION

ZnO has a whole set of properties that are well combined with each other, such as: high optical transparency, the presence of piezo and photo effects, low resistivity, radiation resistance, etc. Zinc oxide is a direct-gap semiconductor with a band gap of 3.36 eV and a high binding energy exciton state ~ 60 MeV. This combination of physical parameters, as applied to ZnO thin films, makes this material promising for creating UV, blue, green, and white LEDs, optical and gas sensors, piezo sensors, HUD displays, transparent contacts, etc.

Semiconductor-ferroelectric structures (ZnO-$LiNbO_3$) are currently attracting much attention of researchers due to the possibility of creating radio photonics and functional microelectronics devices on their basis.

Zinc oxide initially has an electronic type (n-type) conductivity with a fairly low resistivity ($\rho \approx 10^{-3} \div 10^{-4}$ Ω·sm), a high concentration of n-type charge carriers (~ $10^{20} \div 10^{21}$ sm^{-3}), and relatively low mobility ($\mu \approx 5 \div 20$ $sm^2/V \cdot s$) [1].

Lithium niobate can be called a wide gap semiconductor due to the change in the band gap of the crystal (3.4 eV) based on the cross effect. However, due to the high resistivity ($\rho \approx 10^{15} \div 10^{17}$ Ω·sm) and low mobility ($\mu \approx 10^{-3}$ $sm^2/V \cdot s$), as well as the manifestation of spontaneous polarization and hysteresis properties, it belongs to the ferroelectric group of materials.

ZnO nanostructures have a wide range of applications in various devices. ZnO nanorods (NR ZnO) are interesting for their electronic and optoelectronic properties [2,3] and are often functional elements of such devices as ultraviolet (UV) nanolasers, chemical sensors, solar cells, nanogenerators [4,5]. The creation of UV sensors of surface acoustic waves (SAW) based on zinc oxide nanostructures as sensitive elements is a very urgent task; they are promising for economical wireless and batteryless devices [6-8].

In this regard, semiconductor-ferroelectric structures formed on the surface of a ferroelectric substrate from single-crystal lithium niobate make it possible to create optically and electrically controlled structures according to the topology of a field-effect transistor or a field-controlled photoresistor [9]. To create such microdevices, it is necessary to conduct a comprehensive study of the structural, optical, and luminescent properties of semiconductor-ferroelectric structures.

For example, a highly efficient photodetector was developed based on a surfactant generator with a ZnO nanorod layer sensitive to ultraviolet radiation on the surface of a $LiNbO_3$ substrate [10,11]. In particular, the sensor is capable of detecting UV radiation as low as 1.8 $\mu W/sm^{-2}$.

In our work, we present the results of a study of morphological, optical absorption spectra, photoluminescent properties of ZnO-$LiNbO_3$ and ZnO-$LiNbO_3$:Fe structures.

EXPERIMENTAL PART

ZnO were synthesized on a stainless-steel grid by the hydrothermal method [12]. Before growing ZnO nanorods, a seed layer is formed on the surface of the substrates. The dip coating method has been applied to prepare the ZnO seed layer on substrates due to its low cost and simplicity. All reagents (Sigma-Aldrich, 99%) used in the experiment were analytically pure and were used without further purification. Zinc acetate dehydrate ($ZnC_4H_6O_42H_2O$) was dissolved in ethanol with stirring with a stainless-steel shaft mixer at room temperature to obtain a homogeneous solution. The stirred solution is placed in a beaker, the substrates are dipped into the solution at low speed using an automatic dip coating system, and air dried at room temperature.

The growth of ZnO nanorods is carried out in the following sequence: aqueous solutions of zinc nitrate hexahydrate $Zn(NO_3)_26H_2O$ and hexamethylenetetramine $C_6H_{12}N_4$ were prepared. The resulting suspension was transferred to a Teflon

[†] ***Cite as:*** Z.T. Azamatov, Sh.B. Utamuradova, M.A. Yuldoshev, and N.N. Bazarbaev, East Eur. J. Phys. **2**, 187 (2023), https://doi.org/10.26565/2312-4334-2023-2-19

coated stainless steel autoclave. Substrates with a ZnO seed layer were placed on the bottom of the autoclave. Finally, the autoclave was closed and placed in a bath with a water thermostat. The hydrothermal reaction is carried out at 90° C. for 5 hours.

Studies of surface morphology, thickness and elemental composition of the samples were carried out on a scanning electron microscope (SEM) EVO MA10 (Carl Zeiss). The absorption spectra were studied using a Shimadzu UV 3600 spectrometer. The emission spectra of ZnO nanorods were obtained using a photoluminescent setup coupled to a 0.75 μm monochromator with a diffraction grating and highly sensitive photomultipliers. The excitation source was a longitudinally pumped nanosecond pulsed N_2 laser emitting at a wavelength of 337 nm (pulse duration ~6 ns, P ~15 kW, repetition rate 100 Hz). The emission spectra were recorded using a boxcar integrator with a gate width of 40 ns.

RESULTS AND THEIR DISCUSSION

As a result of SEM studies, images of the surface morphologies of grown samples of ZnO-$LiNbO_3$ structures were obtained, which are shown in Fig. 1. At high magnification, ZnO nanorods are clearly visible, with their sizes indicated. A similar picture is shown by the images of the ZnO-$LiNbO_3$:Fe surface, which we do not present.

Analysis of the SEM images of both samples shows that zinc oxide nanorods grow equally on both substrates. It can be seen that the average size of nanorods is 10–20 μm in length and 1–3 μm in diameter.

To measure the thickness of the nanorod layer in SEM, the sample was rotated through an angle of 90° to the surface grown from ZnO Fig. 2. It can be seen that the thicknesses in different parts of the applied layer are in the range of 2-12 μm. Note that, depending on the task, the layer thickness can be changed during its growth.

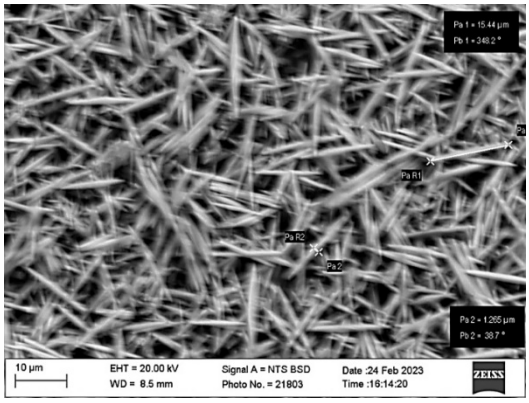

Figure 1. Surface morphology of ZnO-$LiNbO_3$

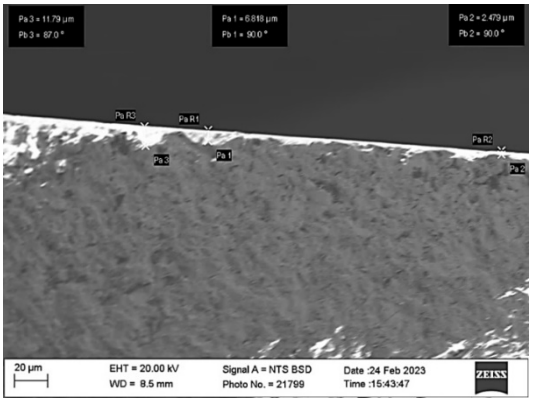

Figure 2. Layer thicknesses of ZnO-$LiNbO_3$ nanorods

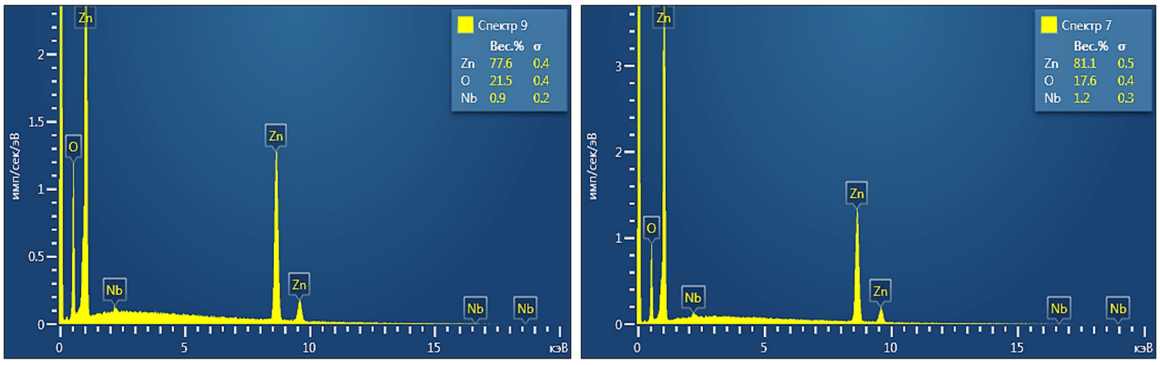

a **b**

Figure 3. Elemental analysis a) ZnO-$LiNbO_3$ and b) ZnO-$LiNbO_3$:Fe

As can be seen from Fig. 3 elemental analysis of the spectra shows the presence and percentage of all components of the structures, the device does not see Fe, due to its low content, which goes beyond the measurement limits of the device.

The photoluminescence spectra of the structures under study are shown in Fig. 4. In both spectra of the structures under study, there is a narrow intense luminescence band located in the UV region, the maximum of which falls in the vicinity of the wavelength – 387 nm. The maximum of the luminescence band corresponding to the ZnO layer hydrothermally deposited on the $LiNbO_3$ surface (Figure 4, curve 1) is at a wavelength of 387 nm and has a half-width of 34 nm.

The maximum of the luminescence band corresponding to the ZnO layer hydrothermally deposited on the $LiNbO_3$:Fe surface (Figure 4, curve 2) is at a wavelength of 390 nm and has a half-width of 32 nm. The intensity of the band in the spectrum of ZnO nanorods grown on a $LiNbO_3$:Fe substrate is 12% less than the intensity of the analogous band in the photoluminescence spectrum for ZnO nanorods grown on a $LiNbO_3$ substrate. The position of the maxima of the narrow UV photoluminescence bands and their spectral half-width suggest that they are similar to the exciton

photoluminescence band [13]. Such a ratio between the intensities of the UV photoluminescence bands of the two samples under study can be explained as follows: the process responsible for intense photoluminescence in the UV spectral range is the recombination of excitons in the bulk of the ZnO layer [14]. The shift of the UV photoluminescence band by 3 nm toward longer wavelengths may be due to the fact that the observed photoluminescence in the zinc oxide layer of nanorods hydrothermally deposited on ferroelectric substrates is the total effect of luminescence from both exciton complexes and deep traps present in the bulk zinc oxide layer of nanorods.

For both structures under study, broad luminescence bands are observed, which lie in the blue-green spectral region of the visible range. These broad photoluminescence bands have similar half-widths and intensities (the spectra merge). The intensities of the broad photoluminescence band of the ZnO-$LiNbO_3$ and ZnO-$LiNbO_3$:Fe structures coincide. Its maximum is at a wavelength of 562 nm, and its half-width is 154 nm. The defects responsible for photoluminescence in this spectral range include oxygen vacancies, which are both electrically and optically active defects. Optically active defects and the spectral position of broad maxima correlate with the literature data [15].

We compared our results with the results obtained in the following works: [16] – ZnO films obtained by laser ablation; [1] – ZnO films obtained by vacuum deposition on $LiNbO_3$ ferroelectric substrates. The first exciton (in the UV spectral region) obtained peak is similar to the peak obtained in our studies from zinc oxide films grown by hydrothermal synthesis. But the peaks of vacancy oxygen in the second visible (blue-green spectral region) do not coincide. In our results, the symmetry of the spectral lines is practically preserved, and the intensities of both peaks are of the same order, no additional peaks are observed.

Studies have shown that grown ZnO nanorods are excited by ultraviolet light, the PL spectrum of ZnO nanorods consists of two peaks: a narrow one in the UV range and a broad emission band in the visible range. The UV peak was attributed to the near edge emission of the band or the free exciton of ZnO, and the blue-green emission to the far luminescence band and vacancy oxygen.

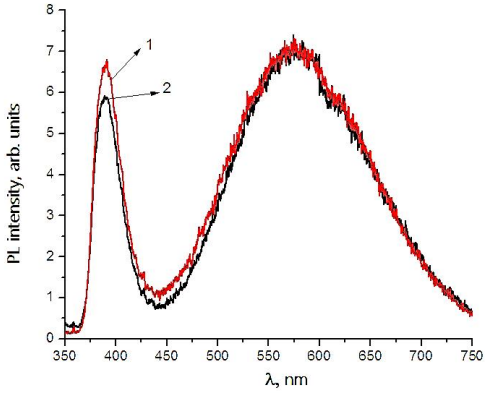

Figure 4. Photoluminescence spectra of structures: ZnO-$LiNbO_3$ (1), ZnO-$LiNbO_3$:Fe (2)

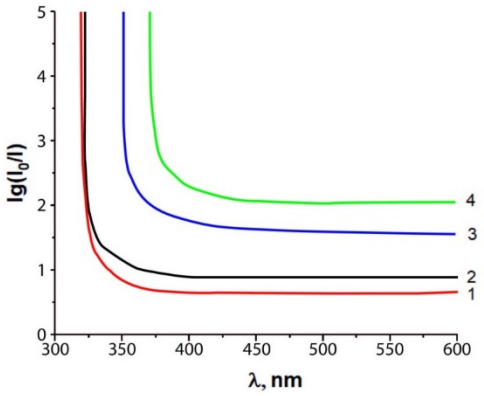

Figure 5. Absorption spectra of structures: ZnO-$LiNbO_3$ (1.2), ZnO-$LiNbO_3$:Fe (3.4)

To study the optical properties of the resulting semiconductor-ferroelectric structures in the UV and visible ranges of the spectrum, studies of the absorption spectra were carried out. The absorption spectra Fig. 5 were studied in the wavelength range from 200 to 900 nm. The parallelism of the spectral lines remains practically unchanged from 400 nm to the near infrared region. Absorption begins to increase rapidly from 400 nm. Therefore, in the figure, the range from the short-wavelength range to 600 nm is taken. absorption spectra were taken from both samples - from the side: ZnO (1.4) and substrates (2.3).

For comparison, the absorption spectra of the samples were measured on both sides. It can be seen from the spectra that in the ZnO-$LiNbO_3$ structure the spectrum taken from the side of the ZnO layer is lower than the spectrum taken from the side of the base (Fig. 5, curve 1). This indicates that the ZnO layer reflects light. But in the ZnO-$LiNbO_3$:Fe structure, on the contrary, the spectrum of the ZnO layer is higher (Fig. 5, curve 4). We can say that this is the effect of Fe ions participating in the structure. The obtained absorption spectrum in the decreasing linear part of the graph was approximated by a straight line up to the intersection with the abscissa axis. The point of intersection of this line with the abscissa axis is the wavelength corresponding to the absorption edge of the crystal. The band gap was determined by the formula:

$$E = \frac{hc}{\lambda} \tag{1}$$

where λ is the wavelength corresponding to the absorption edge, h is Planck's constant, c is the speed of light in vacuum.

The widths of the geometrically defined band gaps E_g are 3.86, 3.85, 3.52, and 3.34 eV, respectively, according to the curves in Fig. 5. The refractive indices are determined by the following imperial formula, taking into account Eg, which is given in [17]:

$$n^2 - 1 = \frac{A}{(E_g + B)^2} \tag{2}$$

where $A = 25E_g + 212$, $B = 0.21E_g + 4.25$, while the changes in the refractive index look, respectively, as follows; 2.20, 2.21, 2.26, 2.30.

CONCLUSION

Thus, it can be said that for all methods of obtaining ZnO nanostructures on pure and iron-doped lithium niobate substrates, the surface morphology is the same, they are covered with ZnO nanoparticles or nanorods (clusters), and, in the elemental composition of nanoparticles, oxygen predominates, and vice versa in nanorods. The results of luminescence analysis show similarity of the spectra both in the UV region and in the blue-green part of the spectrum, but the spectra obtained by us are symmetrical and without additional "peaks", due to a larger amount of interstitial oxygen. In addition, it can be seen that the refractive indices calculated using the above empirical formula are very close to the experimental results of other authors.

ORCID IDs

Sharifa B. Utamuradova, https://orcid.org/0000-0002-1718-1122

REFERENCES

[1] N.M. Lyadov, A.I. Gumarov, R.N. Kashapov, A.I. Noskov, V.F. Valeev, V.I. Nuzhdin, V.V. Bazarov, et al., "Structure and optical properties of ZnO with silver nanoparticles," Physics and technology of semiconductors, **50**(1), (2016).
[2] A.B. Djurišić, and Y.H. Leung, Small **2**, 944-961 (2006). https://doi.org/10.1002/smll.200600134
[3] C.Y. Chen, M.W. Chen, J.J. Ke, C.A. Lin, J.R.D. Retamal, and J.H. He, "Surface effects on optical and electrical properties of ZnO nanostructures," Pure Appl. Chem. **82**, 2055 (2010). http://dx.doi.org/10.1351/PAC-CON-09-12-05
[4] A.K. Zeinidenov, A.K. Abisheva, B.R. Ilyassov, A.K. Aimukhanov, and S.E. Abilmazhinov, "Influence of structural features of zno films on optical and photoelectric characteristics of inverted polymer solar elements," Eurasian Physical Technical Journal, **18**(2), 40-46 2021, https://doi.org/10.31489/2021No2/40-46
[5] Ş. Kaya, "Effect of annealing temperature on structural, electrical, and UV sensingcharacteristics of n-ZnO/p-Si heterojunction photodiodes*,"* Turkish Journal of Physics, **43**(3), 4 2019). https://doi.org/10.3906/fiz-1812-16
[6] A.S. Bagdasarian, V.G. Dneprovski, G.Y. Karapetyan, S.A. Bagdasaryan, in: *Piezoelectric and Related Materials. Research and Applications*, edited by by I.A. Parinov, (Nova Science Publishers, New York, 2012), pp. 189.
[7] P. Sharma, S. Kumar, and K. Sreenivas, "Highly sensitive ultraviolet detector based on ZnO/LiNbO3 hybrid surface acoustic wave filter," Mater J. Res. **18**, 545 (2003). https://doi.org/10.1063/1.1622436
[8] A.A. Mohanan, R. Parthiban, and N. Ramakrishnan, "Shadow mask assisted direct growth of ZnO nanowires as a sensing medium for surface acoustic wave devices using a thermal evaporation method," J. Micromech, Microeng. **26**, 025017 (2016). https://doi.org/1088/0960-1317/26/2/025017
[9] Zh. Wen, Ch. Li, D. Wu, A. Li, and N. Ming, "Ferroelectric-field-effect-enhanced electroresistance in metal / ferroelectric / semiconductor tunnel junctions," Nature Materials. **12**, 617. (2013). https://doi.org/10.1038/nmat3649
[10] D.L. Cheng, K.S. Kao, C.H. Lo, C.H. Liang, L.P. Chan, C.W. Tsung, and Y.Y. Li, "Ultraviolet sensing system using ZnO based surface acoustic wave oscillator," in: *Proceedings of the 3rd International Conference on Industrial Application Engineering*. **435**, (2015), pp. 435-438. https://doi.org/10.12792/iciae2015.076
[11] Wa. Wen-Bo, G. Hang, H. Xing-Li, X. Wei-Peng, C. Jin-Kai, W. Xiao-Zhi, and L. Ji-Kui, "Transparent ZnO/glass surface acoustic wave based high performance ultraviolet light sensors," Chin. Phys. B, 24(5), 057701 (2015). https://doi.org/10.1088/16741056/24/5/057701
[12] R.R. Jalolov, B.N. Rustamova, Sh.Z. Urolov, and Z.Sh. Shaymardanov, "The influence of size on the photoluminescence properties of ZnO nanostructures," Uzbek Journal of Physics, **23**(2), 40-44 (2021). https://doi.org/10.52304/.v23i2.238
[13] B.D. Yao, V.F. Chang, and F. Wang, "Formation of ZnO nanostructures by a simple way of thermal evaporation," Appl. Phys. Lett. **81**, 757 (2002). https://doi.org/10.1063/1.1495878
[14] P. Narin, E. Kutlu, G. Atmaca, A. Atilgan, A. Yildiz, and S.B. Lisesivdin, "Structural and optical properties of hexagonal ZnO nanostructures grown by ultrasonic spray CVD," Optik, **168**, 86-91 (2018). https://doi.org/10.1016/j.ijleo.2018.04.089
[15] A.N. Gruzintsev, V.T. Volkov, "Modification of the electrical and optical properties of the ZnO thin films under the ultraviolet radiation", Physics and technology of semiconductors, **45(11)**, p.1476-1480 (2011). http://journals.ioffe.ru/articles/viewPDF/7556
[16] L.V. Grigoriev, I.S. Morozov, N.V. Zhuravlev, A.A. Semenov, and A.A. Nikitin, "Photoluminescent and photoelectric properties of the ZnO-$LiNbO_3$ thin-film structure in the ultraviolet and visible spectral ranges," Physics and technology of semiconductors, 54(3), (2020). https://www.springerprofessional.de/en/photoluminescence-and-photoelectric-properties-of-the-zno-linbo3/17934476
[17] Z.T. Azamatov, M.A.Yuldoshev, N.N. Bazarbayev, "Effect of gamma irradiation on optical properties of lithium niobate and $LiNbO_3$:Fe crystals," Izvestiya vuzov. Physics, **2**, 106-113 (2023).

ДЕЯКІ ВЛАСТИВОСТІ НАПІВПРОВІДНИКОВО-СЕГНЕТЕЛЕКТРИЧНИХ СТРУКТУР

Закір'ян Т. Азаматов, Шафіра Б. Утамурадова, Муроджон А. Юлдошев, Нурлан Н. Базарбаєв
Інститут фізики напівпровідників та мікроелектроніки Національного університету Узбекистану, вул. Янги Алмазор, 20, Ташкент, Узбекистан

У статті представлені властивості напівпровідникових сегнетоелектричних структур, що складаються з наностержнів ZnO, вирощених при низьких температурах гідротермальним методом на підкладках $LiNbO_3$ та $LiNbO_3$:Fe. Отримані структури аналізували за допомогою скануючого електронного мікроскопа, фотолюмінесценції та спектрофотометрії. СЭМ зображення та спектри; спектри поглинання; спектри фотолюмінесценції в ультрафіолетовому і видимому діапазонах. Дослідження показали можливість використання поряд з іншими гідротермального методу синтезу $Zn(NO_3)_26H_2O$ та $C_6H_{12}N_4$ для отримання масивів наностержнів ZnO як чутливого елемента датчиків УФ-випромінювання на основі ПАР.

Ключові слова: *наностржні; фотолюмінесценція; скануючий електронний мікроскоп; спектр поглинання*